Laurent+Pietarinen partial-wave analysis

A. Švarc*
Rudjer Bošković Institute, Bijenička cesta 54, P.O. Box 180, 10002 Zagreb, Croatia and Tesla Biotech d.o.o., Mandlova 7, 10000 Zagreb, Croatia

R. L. Workman
Institute for Nuclear Studies, Department of Physics, George Washington University, Washington, DC 20052, USA

(Received 15 June 2022; revised 5 June 2023; accepted 11 July 2023; published 26 July 2023)

A new energy-dependent fit strategy, independent of any specific microscopic theory, is applied to kaon photoproduction data with center-of-mass energies ranging from 1625 MeV to 2296 MeV. Experimental data are fitted in terms of a modified Laurent expansion (Laurent+Pietarinen expansion) which previously has been successfully applied to multipoles. The present aim is to extract resonance pole parameters directly from the data, rather than from sets of multipoles. A constrained single-energy fit is then used to search for missing structures. In this proof-of-principle study, the data are well described by the initial L+P fit, and it is shown that only a moderate amount of structure, mostly in higher multipoles, is missing from the original fit. Problems due to an unmeasurable overall phase, plaguing single-channel multipole analyses, are mitigated by implementing a form of phase limitation, fixing the initial values of fit parameters using a multichannel analysis.

DOI: 10.1103/PhysRevC.108.014615

I. INTRODUCTION

Measurements of meson-nucleon scattering and photoproduction, with polarized beams, targets, and recoil particles, have a long history, largely motivated by the search for baryon resonances and their properties. The resulting data have been analyzed and reanalyzed as new measurements and analysis techniques have become available. Most current studies employ elaborate multichannel formalisms that cannot easily be reproduced by experimental groups providing the data. Analysis groups can obtain partial-wave amplitudes and continue these to poles in the complex energy plane but experimental groups, seeking to determine the influence of their measurements, must often rely on less-elaborate methods or fits taken from another group. Differences in these models also introduce systematic errors, complicating the confirmation or comparison of different results. It would be useful to have a single-channel technique available to perform this task. In practice, some minimal phase information from a multichannel analysis is required to avoid the continuum ambiguity in a single-energy analysis. Some ways to implement this multichannel constraint have been explored in Refs. [1,2].

In the present study, a more direct connection between pole parameters and data is developed. This method avoids the construction of an explicit model for the process, instead employing analyticity properties of complex functions in the vicinity of poles and cuts. This approach, the Laurent+Pietarinen (L+P) expansion, provides an approximation to the analytic function under consideration using the Laurent theorem, and represents the regular background term as a fast-converging series in a conformal variable with chosen branch points [3–6]. This method was at first applied to the extraction of poles from partial waves or multipoles [7,8] with notable success [9–12].

However, the main problem with this approach is that it requires having partial waves (multipoles) already at one's disposal. The source may be some theoretical model, or the result of a single-energy partial-wave analysis (SE PWA) which is constrained to be reasonably continuous.[1] Here, the L+P analysis technique is extended to analyze experimental data. Instead of analyzing single multipoles individually, all multipoles are fitted simultaneously. An L+P decomposition of a finite set of multipoles was made and used to reconstruct all available observables. The L+P parameters were then fitted directly to measured data. In this way, complications of a theoretical model were replaced by the selection of terms in the L+P decomposition, the relevant singularities (poles and branch points) of each partial wave. While this is, in principle, a single-step procedure, fitting available data sets with a sufficient number of parameters, the goodness of fit will depend on where one cuts off the L+P expansion. To address this issue, the single-energy fit method is used to search for structure missing in the L+P expansion. As a first proof-of-principle study, a minimal L+P expansion is fitted to kaon photoproduction data, followed by a single-energy fit.

*Corresponding author: svarc@irb.hr

[1]It is well known that any unconstrained single-channel, single-energy partial-wave analysis (SC SE PWA) has discontinuities due to the continuum ambiguity [13,14].

In the next section, the formalism used in the L+P and single-energy fits is outlined. Particular attention is paid to the cutoff in L+P expansion terms and the starting point and constraints used in the fit. Results are then presented to show the fit quality for observables and consistency of the L+P and single-energy amplitudes. Prospects for an enhanced analysis, utilizing a more complete set of L+P parameters, is considered. Finally, some conclusions from this study are listed.

II. FORMALISM

A. Laurent+Pietarinen partial-wave analysis

In Refs. [7,8], a method to analyze the analytic structure of any complex function was formulated. The function, in particular a partial-wave or multipole amplitude, was locally represented in terms of a Laurent decomposition where the regular (nonpole) part was expanded in a sum of finite, rapidly converging power series in a conveniently defined conformal variable (one series per branch point). The most general form used to analyze an analytic function of interest was given by [15]

$$T(W) = \sum_{i=1}^{N} \frac{u_i + \imath\, v_i}{W - W_i} + \sum_{j=1}^{M} \sum_{n=0}^{n^j_{\max}} c_n^j \left(\frac{\alpha_j - \sqrt{x_j - W}}{\alpha_j + \sqrt{x_j - W}} \right)^n , \tag{1}$$

where W is center-of-mass energy, N is the number of poles, W_i, u_i, v_i are pole positions and residues, M is the number of Pietarinen expansions, $n^j_{\max}$ is the number of coefficients in the jth Pietarinen expansion, c_n^j is the real expansion coefficient, and x_i and α_i are branch-point positions and the Pietarinen expansion strengths, respectively. For analyses of Refs. [7,8], we have used three Pietarinen expansions ($M = 3$) with maximum number of Pietarinen coefficients up to six ($n^j_{\max} = 6$), and up to three resonances per partial wave. With these choices, there was very good agreement with the input function, and reliable pole positions and residues could be obtained.

For each partial wave, exactly this form of the expansion could be used to fit experimental data from kaon photoproduction measurements. However, all multipoles should be minimized at the same time, as observables are given as functions of all multipoles. In the Appendix, the relevant formulas for pseudoscalar meson photoproduction are given. Replacing $E_{\ell\pm}$ and $M_{\ell\pm}$ of Eqs. (A1)–(A4) with the L+P parametrization given in Eq. (1), for each multipole, there exists a well-defined system of equations ready to be fitted to data, using formulas given in Table III. The cutoff in partial-wave angular momentum is always an open issue, as each considered process may have a different number of significant partial waves. However, to aid comparison in this work, we take $L_{\max} = 5$, the number of partial waves fitted in the theoretical approach of the Bonn-Gatchina (BG) group [16,17].

In principle, the formalism is well defined with a clear advantage that the pole-fitting parameters are physical quantities for which, from other processes and/or other analyses, one has approximate values. In addition, one knows which branch points could be important for a particular partial wave, and what the threshold behavior should be. However, in reality, fitting the full database with the number of free parameters listed above is not straightforward. For a typical fit of a multipole in pseudoscalar photoproduction in Refs. [7,8], three Pietarinen expansions were used with up to 6 terms each, and up to three resonances. That amounts to as many as $27 + 12 = 39$ parameters per multipole. For a realistic fit, one has to include waves up to least to $L = 5$. Knowing that one has to fit $J = L + 1/2$ and $J = L - 1/2$ electric and magnetic multipoles, this requires 20 multipoles (recalling that M_{0+} and E_{1-} multipoles are unphysical) to get a good fit. Taking into account that certain multipoles couple to the same J^P ($E_{L\pm}$ and $M_{L\pm}$), and hence have the same pole position, one is still left with typically 800 free parameters. There does exist a sufficient number of measurements in the database to obtain a reliable fit (approximately 8000 data points, including many single- and double-polarization quantities), but the complicated nonlinear structure of the fitted formulas results in excessive CPU time [18]. Recalling that one goal is a useful tool for experimentalists, a less CPU-intensive problem was solved for the present proof-of-principle study.

In the simplified L+P PWA, one Pietarinen expansion per multipole was used, instead of three, retaining the dominant background contribution associated with the $K\Lambda$ threshold. The inclusion of resonances was restricted to 4* states quoted in the baryon summary tables of the Particle Data Group (PDG) [15]. This simplifies the background, a quantity which is generally the hardest to fully calculate, and which is usually simplified in a model. The pole complexity remains unchanged. The number of poles contributing to a multipole is generally less than three; often only a single pole is included in Eq. (1). This simplified form of Eq. (1) is used for $T \in \{E_{\ell+}, E_{\ell-}, M_{\ell+}, M_{\ell-}\}$.

With these approximations, the number of multipole background parameters was reduced from 27 to 9 and, with the reduction of pole terms, the number of utilized parameters was about 300. To further accelerate testing, an interpolation method was used on the database. The fit at interpolated values of all observables was performed, using 36 interpolated instead of 121 measured energy points. The interpolation was done in both variables (energy and angle) simultaneously, as described in Refs. [1,2]. This reduced the number of minimization points from 8000 to about 3000, reducing fit times to a manageable 12 CPU hours.

B. Combining simplified energy-dependent and single-energy partial-wave analysis

Experience gained in Refs. [1,2] was used to estimate how much the simplified L+P PWA actually differed from the full solution. In these previous studies, the best single-channel, single-energy multipoles were obtained using constrained PWA in a two-step procedure. In the first step, we obtained reaction amplitudes which fit the data at all energies where measurements were done, and these amplitudes were taken as constraining functions for a constrained SE PWA in the second step. The essential equations governing our two-step amplitude analysis (AA) method from Ref. [1,2] are given be-

low. It has long been known that unconstrained single-energy PWA is discontinuous, because of continuum ambiguities, and so fails to give useful results (discussed in detail in Ref. [14]). Constraints must be applied. A standard approach of constraining a partial wave analysis is to penalize partial waves that stray too far away from each other while simultaneously fitting the set of measured observables:

$$\chi^2(W) = \sum_{i=1}^{N_{\rm data}} w_i \big[\mathcal{O}_i^{\rm exp}(W,\Theta_i) - \mathcal{O}_i^{\rm th}(\mathcal{M}^{\rm fit}(W),\Theta_i)\big]^2 + \lambda_{\rm pen} \sum_{j=1}^{N_{\rm mult}} \big|\mathcal{M}_j^{\rm fit}(W) - \mathcal{M}_j^{\rm th}(W)\big|^2, \tag{2}$$

where

$$\mathcal{M} \stackrel{\rm def}{=} \{\mathcal{M}_0, \mathcal{M}_1, \mathcal{M}_2, \ldots, \mathcal{M}_{N_{\rm mult}}\},$$

statistical weight w_i is defined as the inverse square of observable uncertainties, and $N_{\rm mult}$ is the number of partial waves (multipoles). Here $\mathcal{M}^{\rm fit}$ are fitting parameters and $\mathcal{M}^{\rm th}$ are continuous partial waves (multipoles); $\mathcal{O}^{\rm exp}$ and $\mathcal{O}^{\rm th}$ are respectively the measured and calculated observables. The drawback of such an approach is that one has to use smooth partial waves usually originating from some theoretical model.

The possibility to make the penalty function independent of a particular model was first formulated in the Karlsruhe-Helsinki elastic pion-nucleon scattering analysis, by Höhler in the 1980s [19]. There, partial waves, which are inherently model dependent, are replaced by a penalty function constructed from reaction amplitudes which can be more directly linked to experimental data without any model in the amplitude reconstruction procedure, a point revisited in the next section. This leads to a change from Eq. (2) to

$$\chi^2(W) = \sum_{i=1}^{N_{\rm data}} w_i \big[\mathcal{O}_i^{\rm exp}(W,\Theta_i) - \mathcal{O}_i^{\rm fit}(\mathcal{M}^{\rm fit}(W),\Theta_i)\big]^2 + \mathcal{P},$$

$$\mathcal{P} = \lambda_{\rm pen} \sum_{i=1}^{N_{\rm data}} \sum_{k=1}^{N_{\rm amp}} \big|\mathcal{A}_k(\mathcal{M}^{\rm fit}(W),\Theta_i) - \mathcal{A}_k(\mathcal{M}^{\rm pen}(W),\Theta_i)\big|^2, \tag{3}$$

where $\mathcal{A}_k$ is the generic name for a reaction amplitude (invariant, helicity, or transversity), which is a function of multipoles $\mathcal{M}$ and angles Θ_i. In the present study, we take the penalty functions $\mathcal{A}_k(\mathcal{M}^{\rm pen}(W),\Theta_i)$ to be transversity amplitudes, obtained using multipoles from the simplified L+P PWA. The constraining function in the second step serves to avoid the continuum ambiguity, which makes unconstrained SE PWA discontinuous. It need not be exact; it is enough that it is smooth, and close to the true value. However, it is very difficult to quantify the penalty function coefficient $\lambda_{\rm pen}$. If it is too small ($\lambda_{\rm pen} = 0$) the result will be discontinuous; if it is too large, the results will too closely follow the constraining value. To find an optimum value, we start with very low values, which still give discontinuous results, and increase gradually until these discontinuities disappear. We elaborate on this point below.

This formalism enabled us to develop criteria for improving simplifications made in L+P PWA. To determine how the simplified L+P PWA differs from the full solution, the formalism developed in Refs. [1,2] was modified by replacing SE amplitude-analysis constraining functions with the simplified L+P PWA amplitudes, which are energy dependent and smooth, but do not reproduce the experimental data exactly. Then, using the proposed formalism, we obtain the best SE result. Differences between the energy-dependent (ED) constraining partial waves, obtained by a simplified L+P PWA, and the final SE result, obtained in a constrained PWA, reveal where the analytic simplifications used in simplified L+P PWA are too crude. These differences can be quantified by performing full L+P PWA of obtained multipoles, as given in Refs. [7–12], and then repeating the L+P PWA with improved analytic content. This process could be repeated iteratively to produce an ED solution which is consistent with the SE values.

C. Remarks on phase ambiguity and initial parameters

Observe that the overall energy- and angle-dependent phase remains unconstrained in step 1 of this method. However, the overall phase weakly enters through the choice of initial parameters in the simplified L+P fit of step 1, and is carried on into step 2 via the constraining function. Establishing reasonable initial parameters will impose some restrictions on an otherwise free phase and reasonable initial parameters are extremely important in complicated nonlinear fits. One already has some prior knowledge of the pole parameters entering the L+P fit (it is assumed that they are not far from the PDG [15] values), but the background parameters (thresholds and Pietarinen coefficients) are numerous and less-well determined. Therefore, one must determine the initial values of the remaining Pietarinen coefficients in some way to constrain the phase; otherwise the fit would tend to produce a final phase which disagrees significantly with the phase coming from multichannel unitarity. We do this by fitting the transversity amplitudes obtained from Bonn-Gatchina multipoles [16,17] using the L+P PWA model. These obtained coefficients (Pietarinen and pole parameters) are then used as initial values in the ED L+P fit of experimental data. In this way one starts with a solution whose overall phase is close to the multichannel phase of the BG model [16,17]. This phase will change in the final solution, but only as much as is needed to improve the fit to polarization data which depend on the interference of reaction amplitude phases, and find one out of many possible solutions which is closer to the data than the initial L+P ED fit. As an aside, this is very similar to the phase treatment in the Karlsruhe-Helsinki fixed-t PWA [19–22]. In that fit to elastic pion-nucleon scattering, the overall phase is not mentioned, but is implicitly introduced as the phase of the solution whose Pietarinen parameters are taken as starting values in a fixed-t analysis of data.

D. The $\gamma p \to K^+\Lambda$ database

The $\gamma p \to K^+\Lambda$ database, used in this study, is identical to one fitted in Ref. [2]. In Table I our database is summarized. It

TABLE I. Experimental data from CLAS and GRAAL used in our PWA. Note that the observables C_x and C_z are measured in a rotated coordinate frame [25]. They are related to the standard observables $C_{x'}$ and $C_{z'}$ in the center-of-mass (c.m.) frame by an angular rotation: $C_x = C_{z'}\sin(\theta) + C_{x'}\cos(\theta)$ and $C_z = C_{z'}\cos(\theta) - C_{x'}\sin(\theta)$; see Ref. [17].

Observable	N	$E_{\text{c.m.}}$ (MeV)	N_E	$\theta_{\text{c.m.}}$ (deg)	N_θ	Reference
$d\sigma/d\Omega \equiv \sigma_0$	3615	1625–2295	268	28–152	5–19	CLAS(2007) [25], CLAS(2010) [26]
Σ	400	1649–2179	34	35–143	6–16	GRAAL(2007) [27], CLAS(2016) [28]
T	408	1645–2179	34	31–142	6–16	GRAAL(2007) [27], CLAS(2016) [28]
P	1597	1625–2295	78	28–143	6–18	CLAS(2010) [26], GRAAL(2007) [27]
$O_{x'}$	415	1645–2179	34	31–143	6–16	GRAAL(2007) [27], CLAS(2016) [28]
$O_{z'}$	415	1645–2179	34	31–143	6–16	GRAAL(2007) [27], CLAS(2016) [28]
C_x	138	1678–2296	14	31–139	9	CLAS(2007) [25]
C_z	138	1678–2296	14	31–139	9	CLAS(2007) [25]

has been taken, in numeric form, from the Bonn-Gatchina and George Washington University (SAID) web pages [23,24]; for general details related to the 2-dimensional interpolation and its implementation, see Refs. [1,2]. However, the interpolating/extrapolating stability in the present study is significantly improved with respect to Refs. [1,2]. Observe that, in angular range, not all observables overlap, and for some data groups extrapolations are needed. However, this extrapolation at extreme forward and backward angles can become rather ambiguous if it is completely determined by the fitting software. Therefore, we have introduced additional kinematical constraints to the measured data at the angular limits:

$$\Sigma = P = T = O_{x'} = O_{z'} = C_x = 0 \quad \text{and} \quad C_z = 1 \quad \text{at} \quad \cos\theta = \pm 1. \tag{4}$$

For the differential cross section $d\sigma/d\Omega$, the Bonn-Gatchina theoretical values were used as a constraint at these angles. This stabilizes the extrapolations at low and high angles significantly, and enables us to increase the angular range from experimentally measured $-0.7 < \cos\theta < 0.8$ to a broader $-0.9 < \cos\theta < 0.9$, and this notably increases the reliability of partial-wave reconstruction.

E. The fit procedure

We propose a two-step procedure. Step 1 is the simplified L+P PWA ED fit of the data which obtains an energy-dependent overall representation of the data in terms of partial waves with well known poles and cuts, and step 2 is the criteria for finding missing resonances and/or improving analytic complexity of the background terms by using the constrained SE PWA technique, and finding where simplified analytic structure is insufficient.

The step 1 fit procedure (simplified L+P PWA ED fit) constitutes a proof-of-principle study, utilizing fewer parameters than have been used in previous pole extractions involving single multipoles. However, this simplification still retains a realistic complexity of the analytic structure, but reduces the number of free parameters. As far as background is concerned, the simplification procedure takes only one L+P expansion point, instead of three, and this branch point is fixed to the pion production threshold. With the intention to keep a minimal number of poles, we retained only one pole per multipole, with the exception of those multipoles where the presence of the second pole is clearly established in the multichannel fits of the Bonn-Gatchina group (S-wave only) PDG [15]. The chosen selection of poles is listed in Table II.

As a large number of parameters is used, we have to carefully select initial parameters for poles and Pietarinen coefficients as this is essential for the success of the fit. To accomplish this, Bonn-Gatchina transversity amplitudes were fitted with the simplified analytic structure described above. To simplify the problem further, all poles which showed signs of having little influence, or even being redundant[2] (negative width, small residue, ...), were disregarded. Very good and stable results in this preliminary fitting of Bonn-Gatchina results were obtained. The obtained parameters, which almost perfectly reproduce Bonn-Gatchina multipoles, were used as initial values in the simplified L+P PWA. The fit to the described experimental database, in the energy range 1625 MeV $< W <$ 2296 MeV and angular range $-0.9 < \cos\theta < 0.9$, required acceptable CPU times of about 12–14 hours. The result of this simplified L+P minimization is a set of multipoles which fit the data better than the ED theoretical model, and are by definition smooth.

As a step 2, the procedure to constrain single-channel, single-energy partial-wave analysis, defined in Refs. [1,2], was applied with the aim to gauge the influence of simplifications to the L+P analysis. Transversity amplitudes were obtained from the smooth multipoles of the simplified L+P PWA, as given by Eqs. (A1)–(A8), and used as constraining functions in the constrained SE PWA. The penalty factor λ_{pen} introduced in Eq. (3) is optimized in a way to ensure that the obtained multipoles are still smooth, and the penalty function contribution to the total χ^2 is no larger than 10% (for a full explanation see Refs. [1,2]). This combination of requirements resulted in $\lambda = 150$.

The final result, which is in quality identical to the result given in Refs. [1,2], was obtained. A slightly different phase was found, as the constraining functions do not have the exact Bonn-Gatchina phase that they did in

[2]The poles which Bonn-Gatchina reports are the result of a multichannel fit, so it is a realistic possibility that some of these poles couple weakly to the $K\Lambda$ channel, and so their influence in this channel could be low.

TABLE II. With ReM_i and ImM_i, $i = 1, 2, 3$, we denote pole parameters for simplified L+P PWA and full L+P PWA in GeV units. BP_1^{LP} and BP_2^{LP} denote the fixed πN threshold and the second, effective branch points of Pietarinen expansions, also in GeV units. Numbers in parentheses denote the last digit uncertainty. Bolded numbers for each partial wave are Bonn-Gatchina values from the PDG (the value marked with * denotes one resonance which is demanded by the final L+P PWA fit of the 2+ multipole and which is not given by the PDG [15]). The second row is the result of fitting Bonn-Gatchina transversity amplitudes with the simplified L + P PWA. The third row shows the result of the simplified L + P ED PWA fit, and the fourth row, where it exists, shows the results of the full L + P fit on the final SE AA/PWA amplitudes.

$\ell\pm$	J^P		ReM_1	ImM_1	ReM_2	ImM_2	ReM_3	ImM_3	BP_1^{LP}	BP_2^{LP}
0+	$\frac{1}{2}^-$	**BG poles**	**1.658**	**0.051**	**1.906**	**0.05**				
		Fitted BG amp.	1.667(3)	0.044(3)	1.881(5)	0.088(4)			1.086	
		L+P ED PWA	1.667(4)	0.044(2)	1.880(5)	0.041(5)			1.086	
		Full L+P	1.688(2)	0.073(1)	1.869(1)	0.043(1)			1.086	
1+	$\frac{3}{2}^+$	**BG poles**	**1.660**	**0.250**	**1.945**	**0.077**				
		Fitted BG amp.			1.904(5)	0.105(5)			1.086	
		L+P ED PWA			1.933(8)	0.067(8)			1.086	
		Full L+P			1.930(1)	0.063(1)			1.086	1.608
2+	$\frac{5}{2}^-$	**BG poles**	**1.654**	**0.075**	**2.040**	**0.195**				
		Fitted BG amp.			2.063(4)	0.256(5)			1.086	
		L+P ED PWA			2.098(14)	0.093(13)			1.086	
		Full L+P	1.671(4)	0.318(4)	2.070(10)	0.093(16)	**1.888(16)***	**0.072(31)***	1.086	1.562
3+	$\frac{7}{2}^+$	**BG poles**			**2.030**	**0.12**				
		Fitted BG amp.			2.056(10)	0.059(10)			1.086	
		L+P ED PWA			2.059(20)	0.040(20)			1.086	
4+	$\frac{9}{2}^-$	**BG poles**			**2.195**	**0.235**				
		Fitted BG amp.			2.113(105)	0.196(114)			1.086	
		L+P ED PWA			2.017(100)	0.180(111)			1.086	
1−	$\frac{1}{2}^+$	**BG poles**	**1.697**	**0.042**	**1.875**	**0.0165**				
		Fitted BG amp.	1.717(3)	0.051(3)					1.086	
		L+P ED PWA	1.710(11)	046(12)					1.086	
		Full L+P	1.694(5)	0.057(3)	1.883(6)	0.056(6)			1.086	1.461
2−	$\frac{3}{2}^-$	**BG poles**	**1.770**	**0.21**	**1.860**	**0.1**	**2.11**	**0.17**		
		Fitted BG amp.					2.109(30)	0.195(30)	1.086	
		L+P ED PWA					2.015(23)	0.094(23)	1.086	
		Full L+P	1.691(1)	0.016(1)	1.806(2)	0.013(9)	2.158(5)	0.088(9)	1.086	0.94
3−	$\frac{5}{2}^+$	**BG poles**	**1.675**	**0.056**	**1.830**	**0.125**	**2.03**	**0.24**		
		Fitted BG amp.					2.013(12)	0.135(11)		
		L+P ED PWA					2.187(227)	0.274(300)	1.086	
4−	$\frac{7}{2}^-$	**BG poles**					**2.150**	**0.165**		
		Fitted BG amp.			1.829(80)	0.154(81)			1.086	
		L+P ED PWA			1.862(889)	0.322(808)			1.086	
5−	$\frac{9}{2}^+$	**BG poles**					**2.150**	**0.22**		
		Fitted BG amp.					1.969(20)	0.105(20)	1.086	
		L+P ED PWA					2.163(220)	0.273(200)	1.086	

Refs. [1,2]. In spite of being close to the smooth result of the simplified L+P minimization, the obtained discrete set of multipoles is an improvement, in terms of the agreement with data.

In comparing discrete multipoles of AA/PWA with the smooth values obtained in simplified L+P PWA (see Figs. 1 and 2) one sees that some discrete sets have more structure than the present simplified L+P version, so the simplified L+P PWA can be improved. This difference is quantified by applying the full L+P PWA of Refs. [7–12] to the obtained SE solutions. As a result, we obtained quantitative information about the effect of missing poles, and multipoles where the

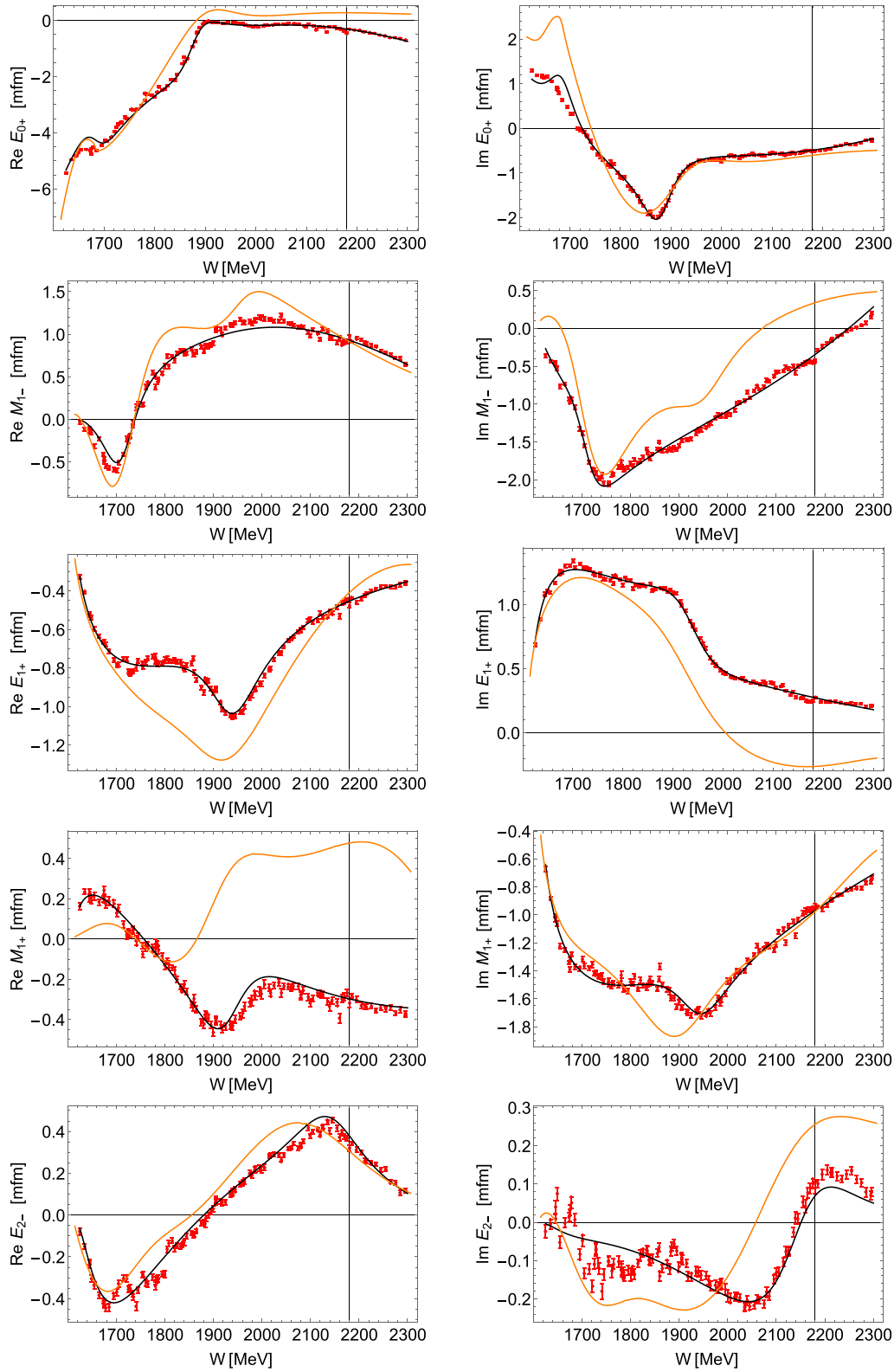

FIG. 1. The multipoles for the $L = 0$, 1, and 2 partial waves. Red discrete symbols correspond to our step 2 SE AA/PWA solution, the black full line gives the result of the step 1 L+P ED PWA, and the full orange line gives the BG2017 ED solution for comparison. The thin vertical black line marks the energy beyond which only 4 observables are measured instead of 8 (cf. Table I).

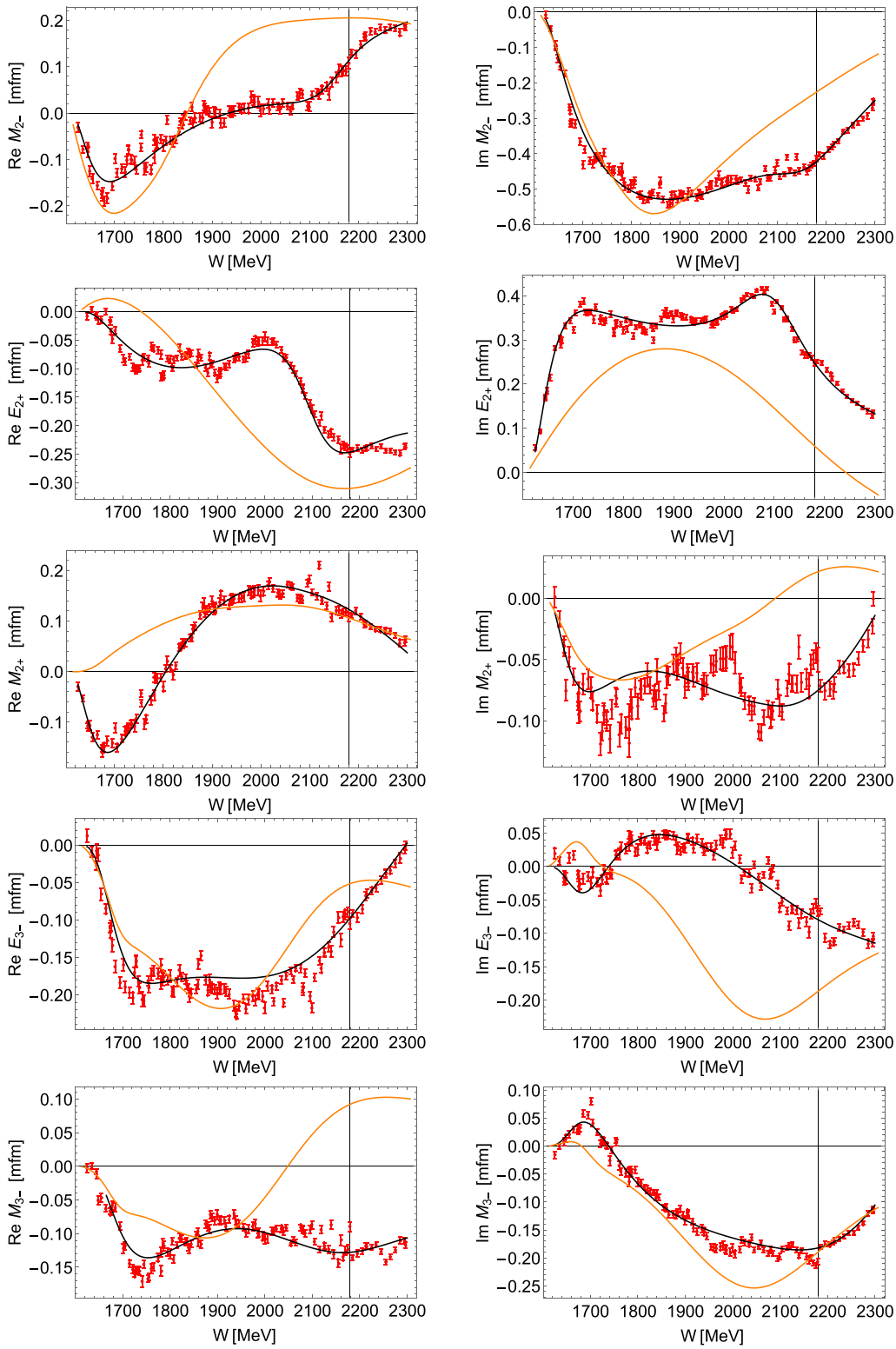

FIG. 2. The multipoles for the $L = 2$ and 3 partial waves. Red discrete symbols correspond to our step 2 SE AA/PWA solution, the black full line gives the result of the step 1 L+P ED PWA, and the orange full line gives the BG2017 ED solution for comparison. The thin vertical black line marks the energy beyond which only 4 observables are measured instead of 8 (cf. Table I).

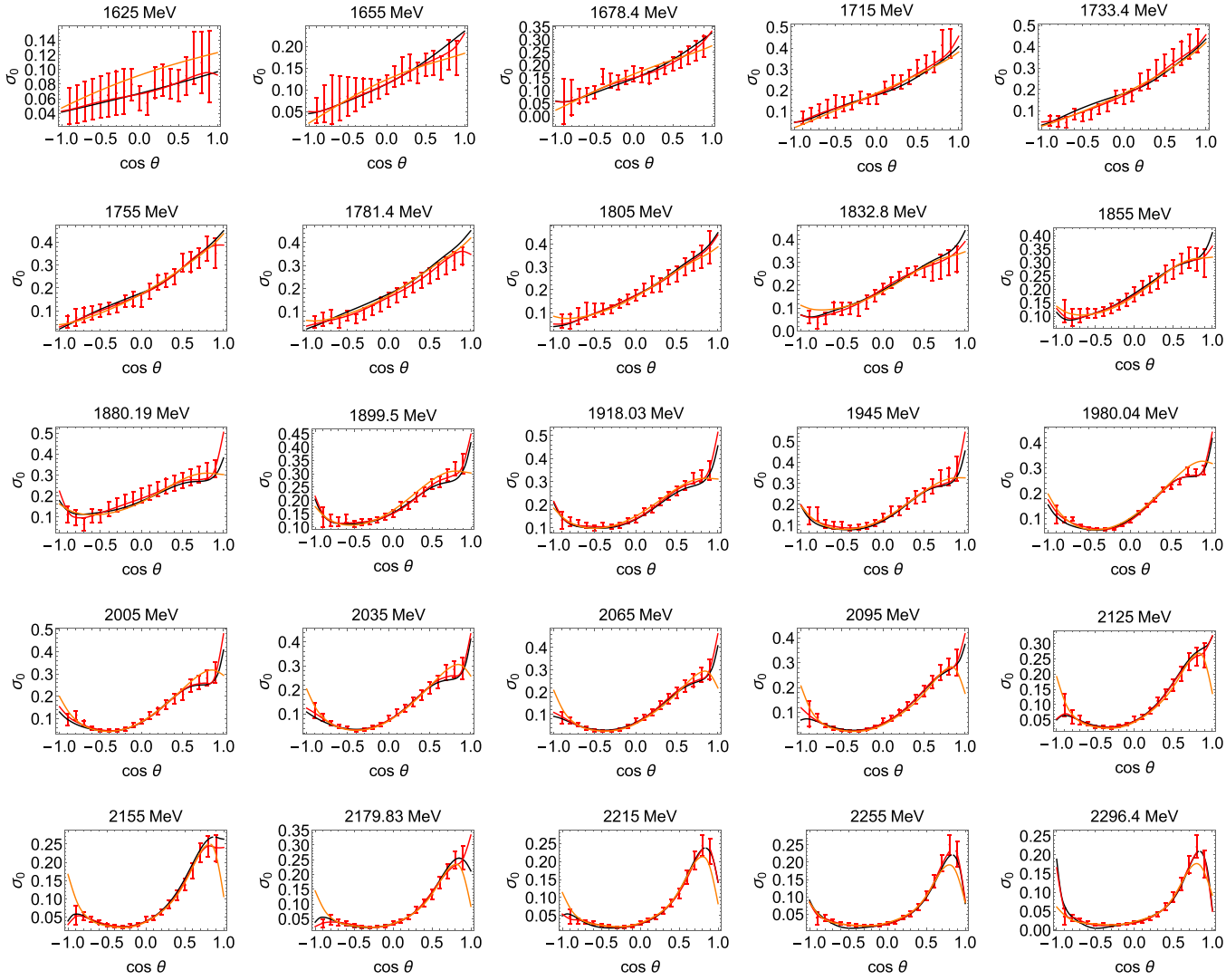

FIG. 3. Comparison of experimental data for σ_0 (red discrete symbols) with results from our SE AA/PWA (red full line), with our L+P ED PWA (black full line), and with the BG2017 fit (orange line) at representative energies.

background structure is inadequate. This is summarized in Table II, where differences in the number of poles in rows denoted by L+P ED PWA and Full L+P indicate multipoles where improvement is needed.

In future studies, a development can be imagined where faster minimization software is used (MINUIT in FORTRAN 90, for example, instead of the presently used Mathematica 11.0, which is known not to be ideal for minimizations) and applied with improved hardware. This would reduce CPU time and enable the introduction of more complex analytic forms (more poles, more Pietarinen expansions having more terms than were used in the simplified L+P expansion). In principle, the present iterative two-step procedure could then be replaced by a more elaborate single-step L+P fit.

F. Error analysis

In the present study, the emphasis is centered on a "fit" to find L+P parameters. However, a quantification of the uncertainty associated with these parameters is extremely important and also required as knowing the best-fit values is only a part of parameter estimation. In the present approach, the error analysis is limited to obtaining statistical errors only. These are fairly reliable, as measured data with realistic errors are fitted. In Table II the last digit uncertainty is given in parentheses. One can see that the confidence level of our result (row denoted by L+P ED PWA) is fairly high for the lowest resonances, but drops notably for higher ones. However, the large number of parameters suggests that we may be facing a situation where local minima are very often encountered. This cannot be controlled within the present approach. However, there are other methods which could be eventually applied like standard techniques such as bootstrapping and Markov chain Monte Carlo (MCMC) (for recent application see Ref. [29]). Currently, parameters found in a Bonn-Gatchina PWA are used as starting points, but these could as well be the starting points of MCMC sampling. However, due to the complexity of formula and large CPU usage, the computational aspects of these attempts could be quite demanding. So, this remains to be done when the calculational improvements are implemented.

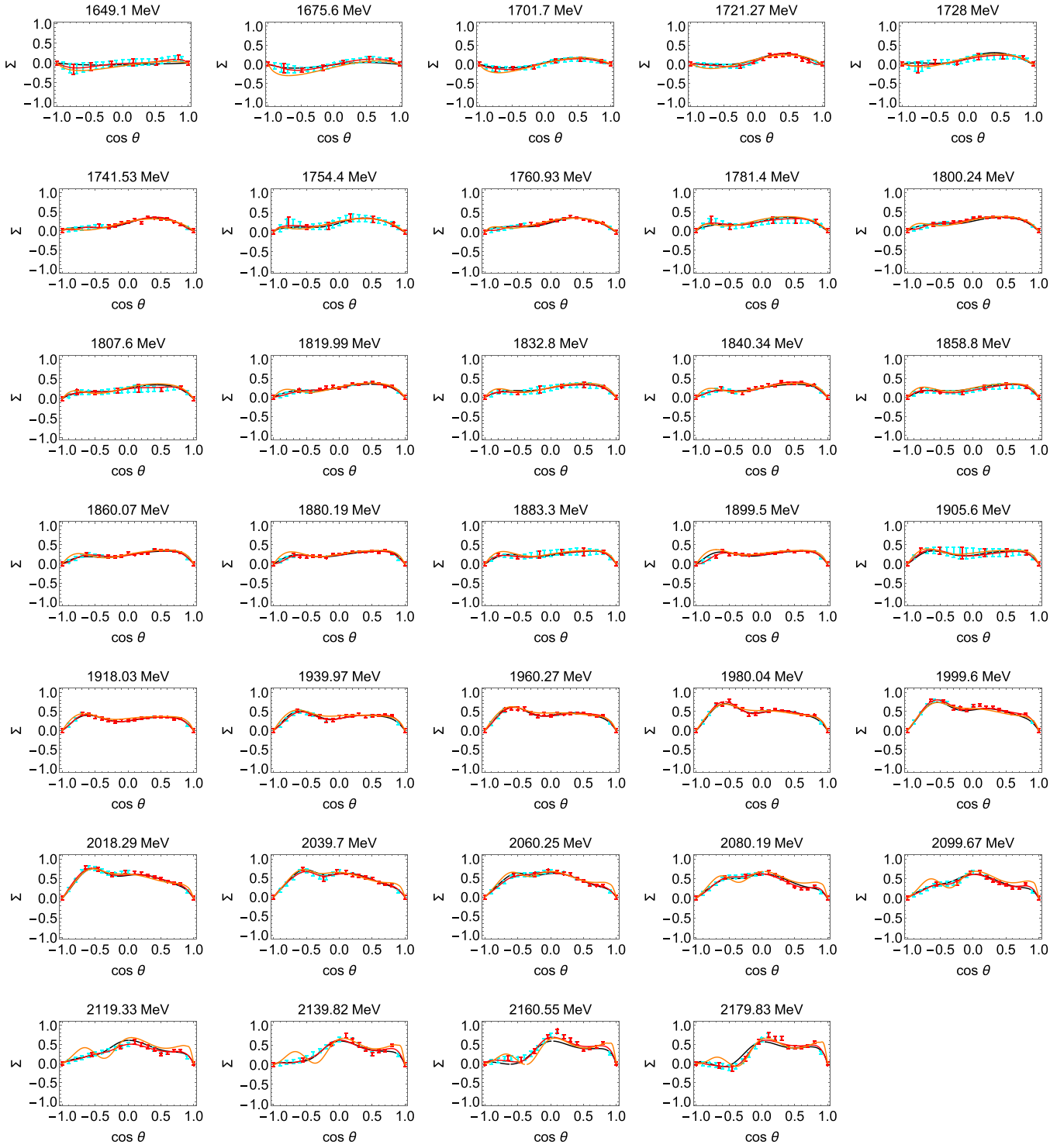

FIG. 4. Comparison of experimental data for Σ (red discrete symbols are measured values and cyan symbols are interpolated values) with results from our SE AA/PWA (red full line), with our L+P ED PWA (black full line), and with the BG2017 fit (orange line) at representative energies.

III. RESULTS FROM THE SIMPLIFIED L+P ED AND SE AA/PWA ANALYSES

In Figs. 1 and 2, we show the final results for multipoles over the full set of energies. Red symbols give the values of multipoles for our step 2 SE AA/PWA solution, which scatter around the black full line produced using the simplified ED L+P fit. Note that this scatter of the SE points is limited by the penalty function and results in a better fit to data. The SE and ED multipoles show better agreement in Fig. 1 for the lower and dominant multipoles; more variation is seen in the higher multipoles of Fig. 2. For comparison, the full

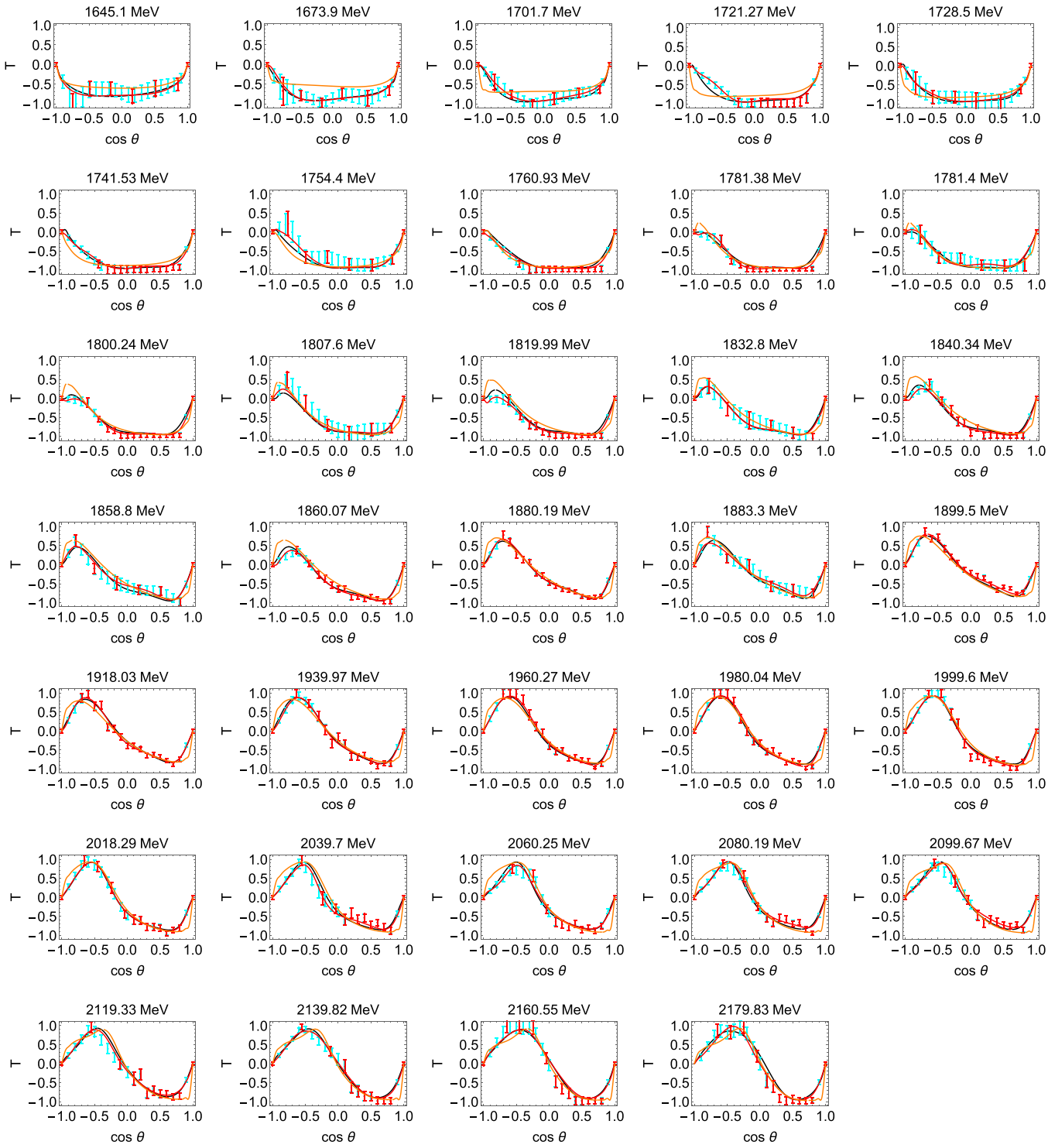

FIG. 5. Comparison of experimental data for T (red discrete symbols are measured values and cyan symbols are interpolated values) with results from our SE AA/PWA (red full line), with our L+P ED PWA (black full line), and with the BG2017 fit (orange line) at representative energies.

orange line gives the BG2017 solution [23] used to initialize the L+P fit parameters. For lower multipoles, the orange and black lines show qualitative agreement, apart from the real part of M_{1+}. Closer agreement should not be expected as the Bonn-Gatchina fits simultaneously account for channels beyond kaon photoproduction. Note that the vertical black line in Fig. 1, indicating the energy where the number of measured observables drops from 8 to 4, is not reflected in jumps to equivalent solutions for the SE AA/PWA points, ostensibly due to the penalty function constraint. Some discontinuities do begin to appear in the higher multipoles of Fig. 2.

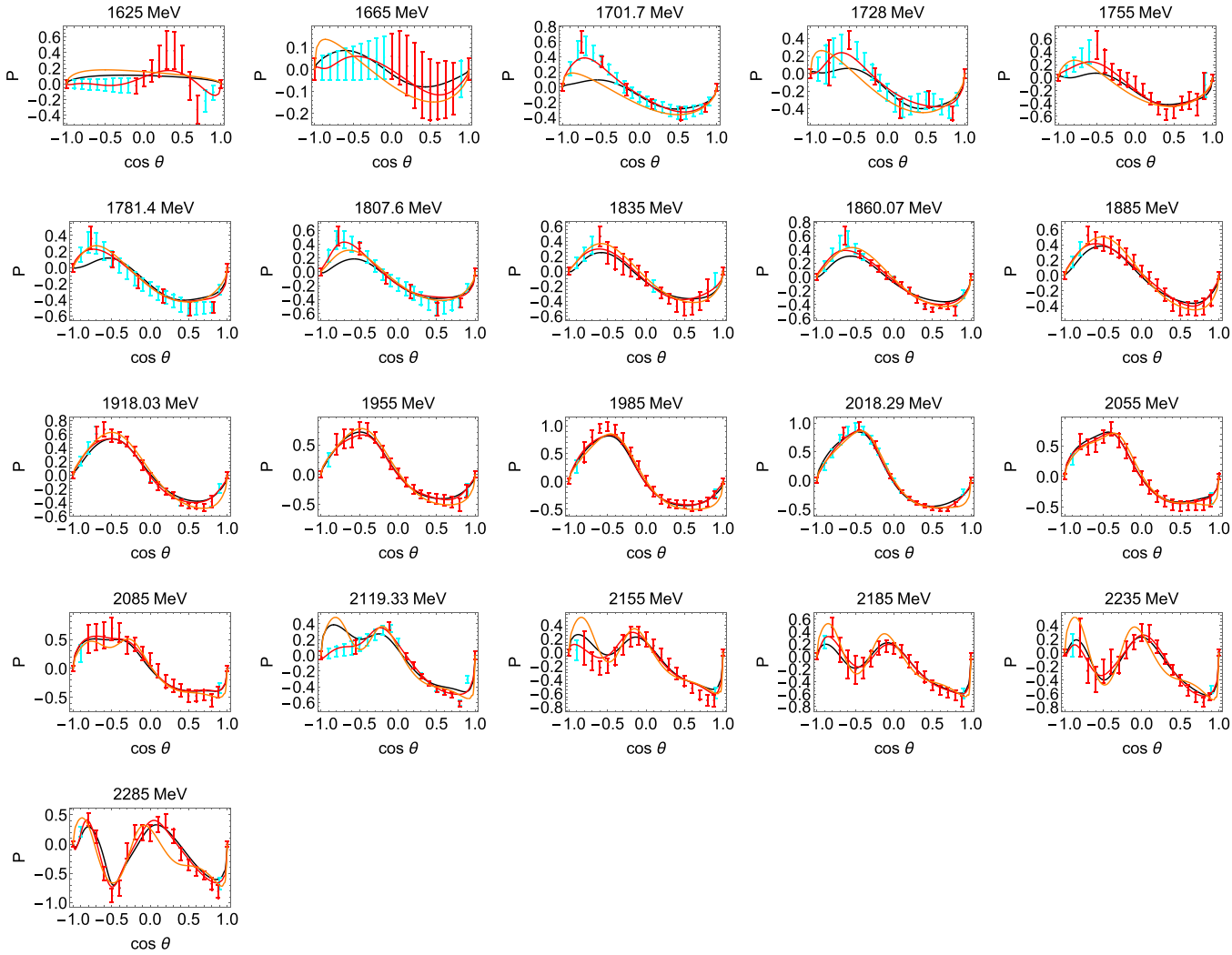

FIG. 6. Comparison of experimental data for P (red discrete symbols are measured values and cyan symbols are interpolated values) with results from our SE AA/PWA (red full line), with our L+P ED PWA (black full line), and with the BG2017 fit (orange line) at representative energies.

In Figs. 3–10, the fits to measured observables resulting from our simplified L+P PWA (black line) and SE AA/PWA method (red full line) are given, as well as predictions from the ED BG2017 solution [23] (full orange line) at representative energies only. All further energies are available upon demand. Red symbols represent the actually measured data points as given in references collected in Table I, and cyan symbols denote the interpolated values obtained with the procedure described in Sec. II D. Here we see that all curves give a good representation of the data, where it has been measured. Some small deviations exist mainly at extreme forward and backward angles where experimental coverage is incomplete. Sharp structures in these regions are influenced by higher partial waves and may be linked to some deviations seen in the multipoles of Fig. 2.

IV. FULL L+P ANALYSIS OF THE (STEP 2) SE AA/PWA MULTIPOLES

It is natural to explore the full analytic structure of the improved SE solutions displayed in Figs. 1 and 2. This can be done if the full L+P method of Refs. [7–12] is applied. In Table II and in Figs. 11 and 12 we show the results.

We see that, for the lowest multipole E_{0+}, the pole positions and the general shape of the multipole, comparing Fig. 1 and Fig. 11, do not change significantly; they are well reproduced with the simplified L+P ED PWA. However, already for the $1-$ and $1+$ multipoles, the shape of the function in Fig. 11 is slightly different from the shape given in Fig. 1. For multipoles $1+$, a second Pietarinen expansion has been added to compensate, and for multipole $1-$, a second resonance and a second Pietarinen expansion have been added. All results are collected in Table II and in Fig. 11. Note that here, effective branch points are employed to represent all branch-cut contributions simultaneously (see Refs. [7–12]).

V. SUMMARY AND CONCLUSIONS

For the first time, pole parameters have been used directly as fitting parameters in an ED L+P analysis of photoproduction data. Previous L+P fits have been applied to sets

FIG. 7. Comparison of experimental data for $O_{x'}$ (red discrete symbols are measured values and cyan symbols are interpolated values) with results from our SE AA/PWA (red full line), with our L+P ED PWA (black full line), and with the BG2017 fit (orange line) at representative energies.

of multipoles obtained in independent analyses of data. As a proof-of-principle calculation, a simplified ED L+P PWA formalism was used, having a reduced number of nonpole parameters and dropping weakly coupled poles. Phase information from the multichannel Bonn-Gatchina analysis was used to weakly mitigate the continuum ambiguity, plaguing single-channel fits. Here we have used the Bonn-Gatchina analysis to initialize the L+P parameters used in the fit to data. To search for missing structure, as a second step, a constrained SE AA/PWA was performed with the result of an L+P ED PWA fit used as a constraint. A comparison of multipoles, from the ED and constrained SE fits, to those from

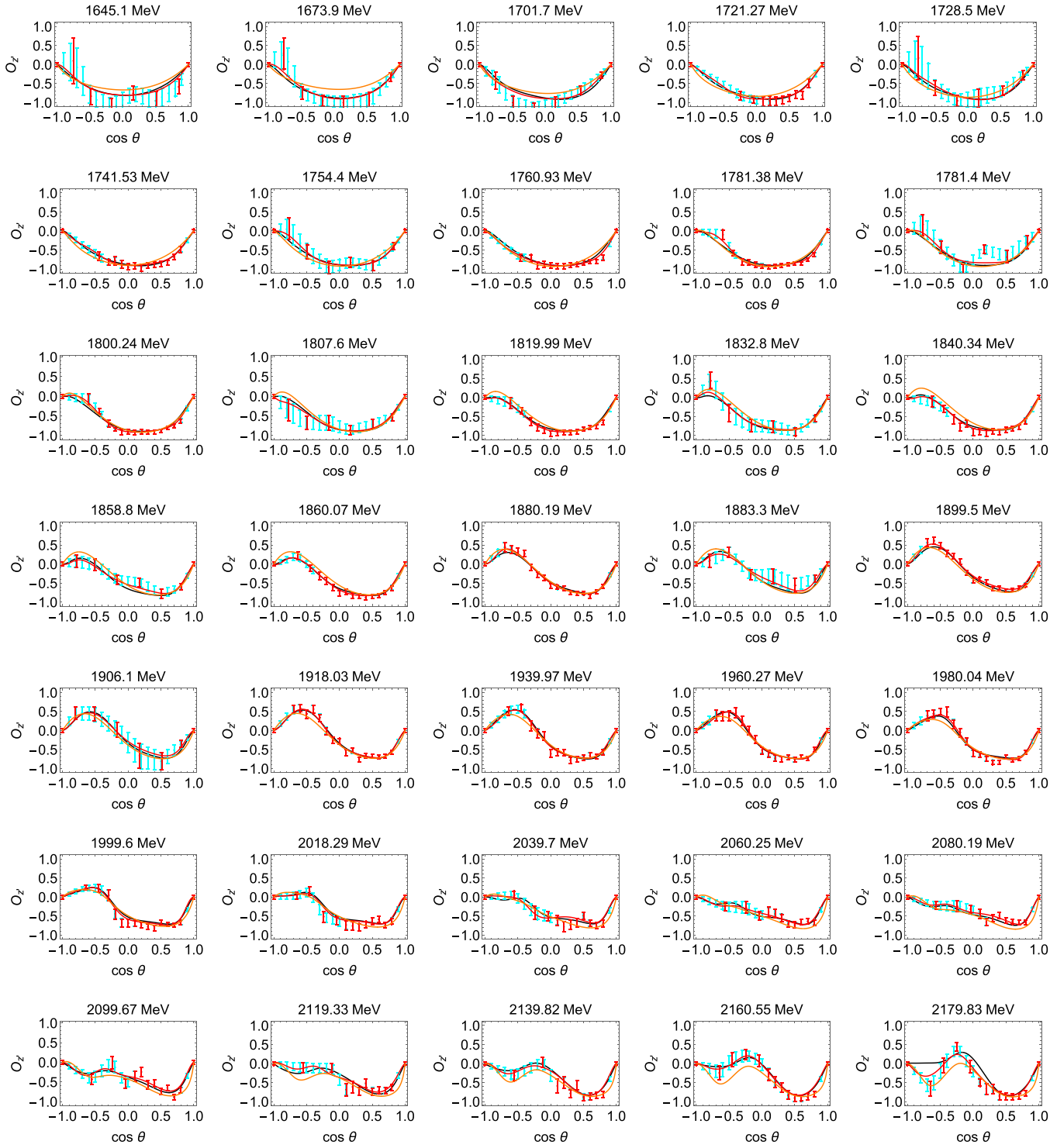

FIG. 8. Comparison of experimental data for $O_{z'}$ (red discrete symbols are measured values and cyan symbols are interpolated values) with results from our SE AA/PWA (red full line), with our L+P ED PWA (black full line), and with the BG2017 fit (orange line) at representative energies.

Bonn-Gatchina, showed reasonable agreement for the largest multipoles but significant deviations from the Bonn-Gatchina analysis in other cases. Closer agreement should not be expected.

To quantify the difference between our simplified L+P ED PWA and the constrained step 2 discrete SE AA/PWA multipoles, which fit the data notably better, we have performed a full L+P analysis of the latter using the formalism of Refs. [7–12] and compared the obtained poles. We conclude that for the dominant E_{0+} multipole no corrections are needed; however all other multipoles are consistent with having at least one more pole and required one extra Pietarinen

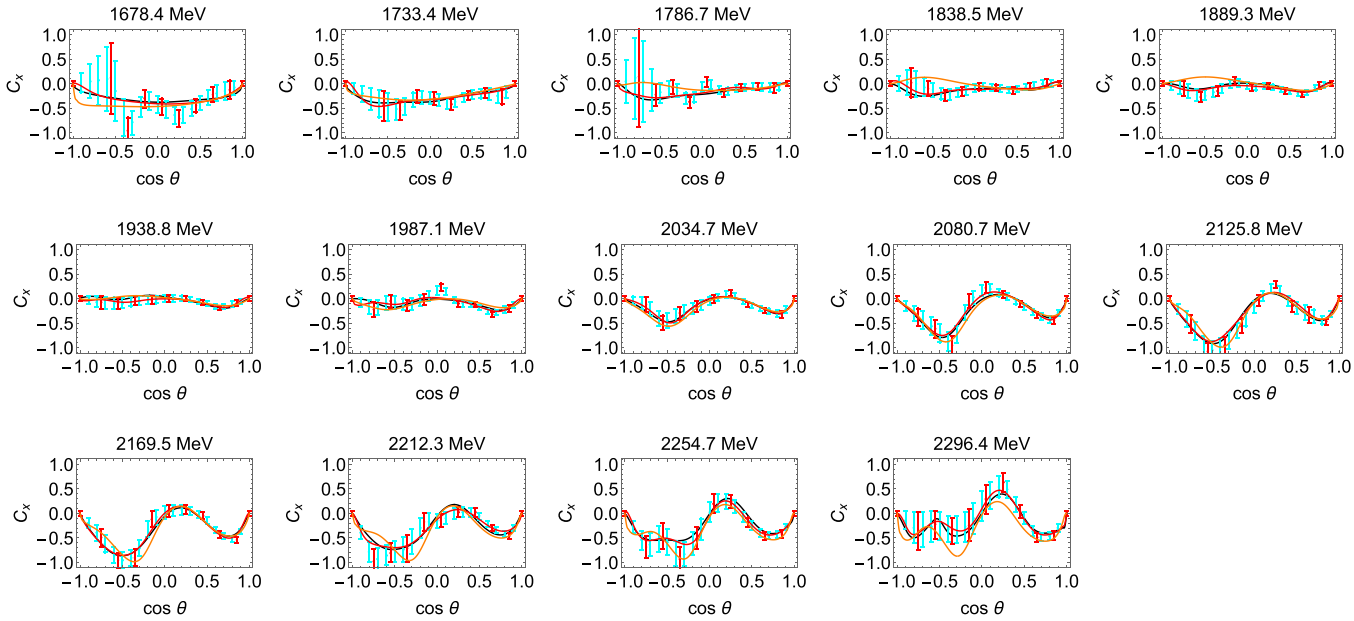

FIG. 9. Comparison of experimental data for C_x (red discrete symbols are measured values and cyan symbols are interpolated values) with results from our SE AA/PWA (red full line), with our L+P ED PWA (black full line), and with the BG2017 fit (orange line) at representative energies.

expansion. Thus, some improvement of analytic structure of simplified L+P ED PWA is needed in future studies.

In the full L+P analysis we encountered one surprising result: In 2+ multipoles, the final fit required an extra resonance with parameters $1.888 + i\,0.072$ GeV, not listed by the PDG. However, this could disappear once the above-mentioned improvements to the L+P structure are implemented.

Some problems of principle remain to be fully addressed. The number of measurements required for a "complete experiment" or a truncated partial-wave analysis continues to be discussed. This has some impact on the ability to perform SE analyses, though arguments generally must ignore the effect of experimental uncertainties. Here, by using a penalty function, our SE results are relatively smooth and tied to an ED solution. However, some indications of a discontinuity where

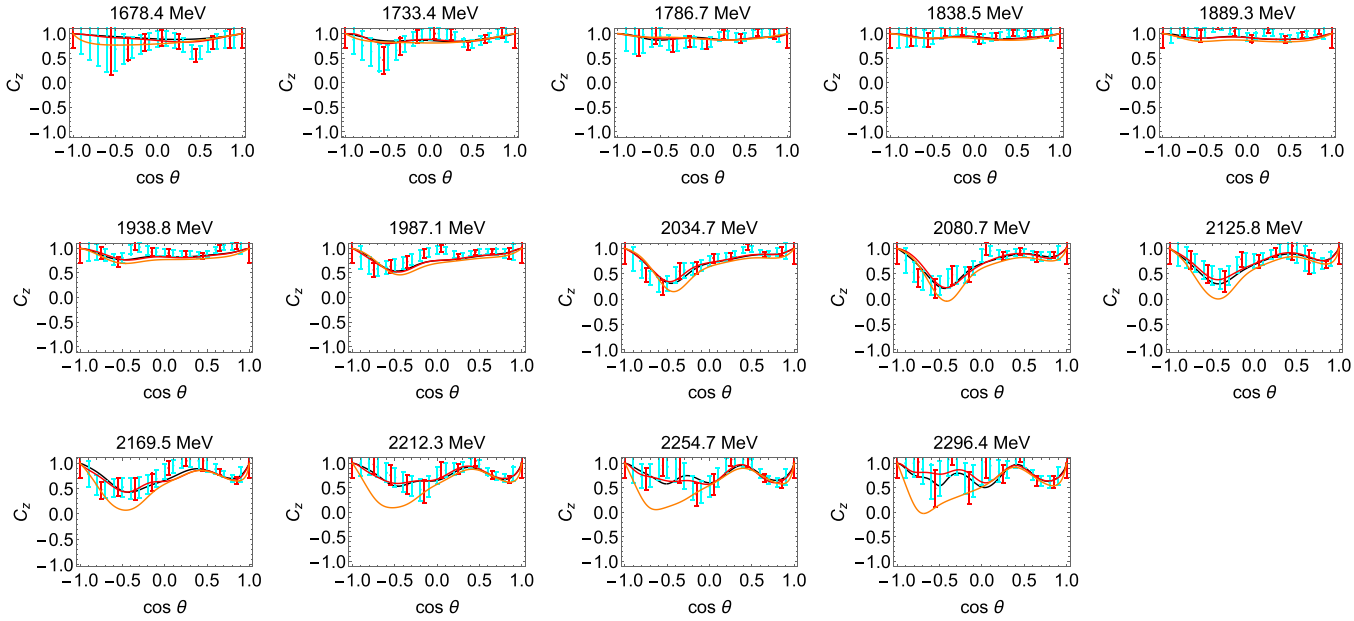

FIG. 10. Comparison of experimental data for C_z (red discrete symbols are measured values and cyan symbols are interpolated values) with results from our SE AA/PWA (red full line), with our L+P ED PWA (black full line), and with the BG2017 fit (orange line) at representative energies.

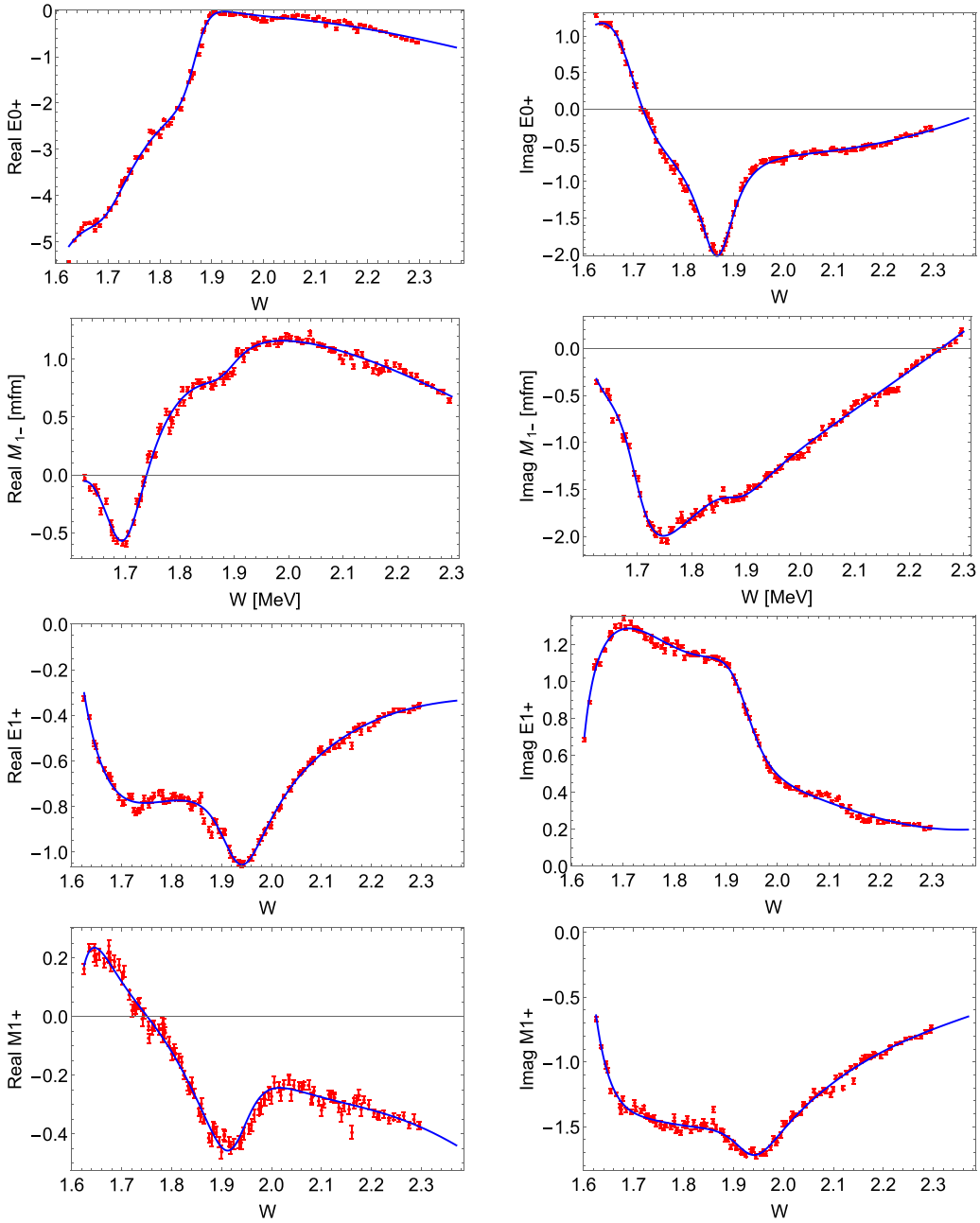

FIG. 11. Multipoles obtained from full L+P PWA of SE AA/PWA solutions. Red symbols are SE AA/PWA final results, and full blue line is the L+P fit. Pole results are given in Table II.

the number of observables changes from 8 to 4 may be visible in the higher multipoles shown in Fig. 2. The main problem of SC methods is that a phase ambiguity [13] remains, but is "hidden" in the choice of initial parameters of our step 1 fit (fitting an analytically simplified L+P expansion of multipoles to the experimental data). Being an overall phase, having no effect on observables, it is difficult to study. However, it can change the appearance of multipoles and therefore is an added problem in comparing the results of different groups. In future, an upgrade of this proof-of-principle calculation will be implemented. As is commonly known, the presently used Mathematica software is notoriously inefficient for the minimization tasks, as the process involves inverting very large matrices, requiring a large amount of memory and CPU time. Other, faster minimization software will be used (MINUIT in FORTRAN90, for example), and applied with the new, better hardware. This will reduce CPU time, and will enable the introduction of more complex analytic forms (more poles, more Pietarinen expansions, and more Pietarinen terms in a single expansion). Hence, the proposed iterative procedure will be fully implemented to formulate the final, full-scale model with the inclusion of error uncertainties and data consistency.

ACKNOWLEDGMENTS

Deepest thanks go to our colleagues Lothar Tiator and Yannick Wunderlich who significantly contributed to an early

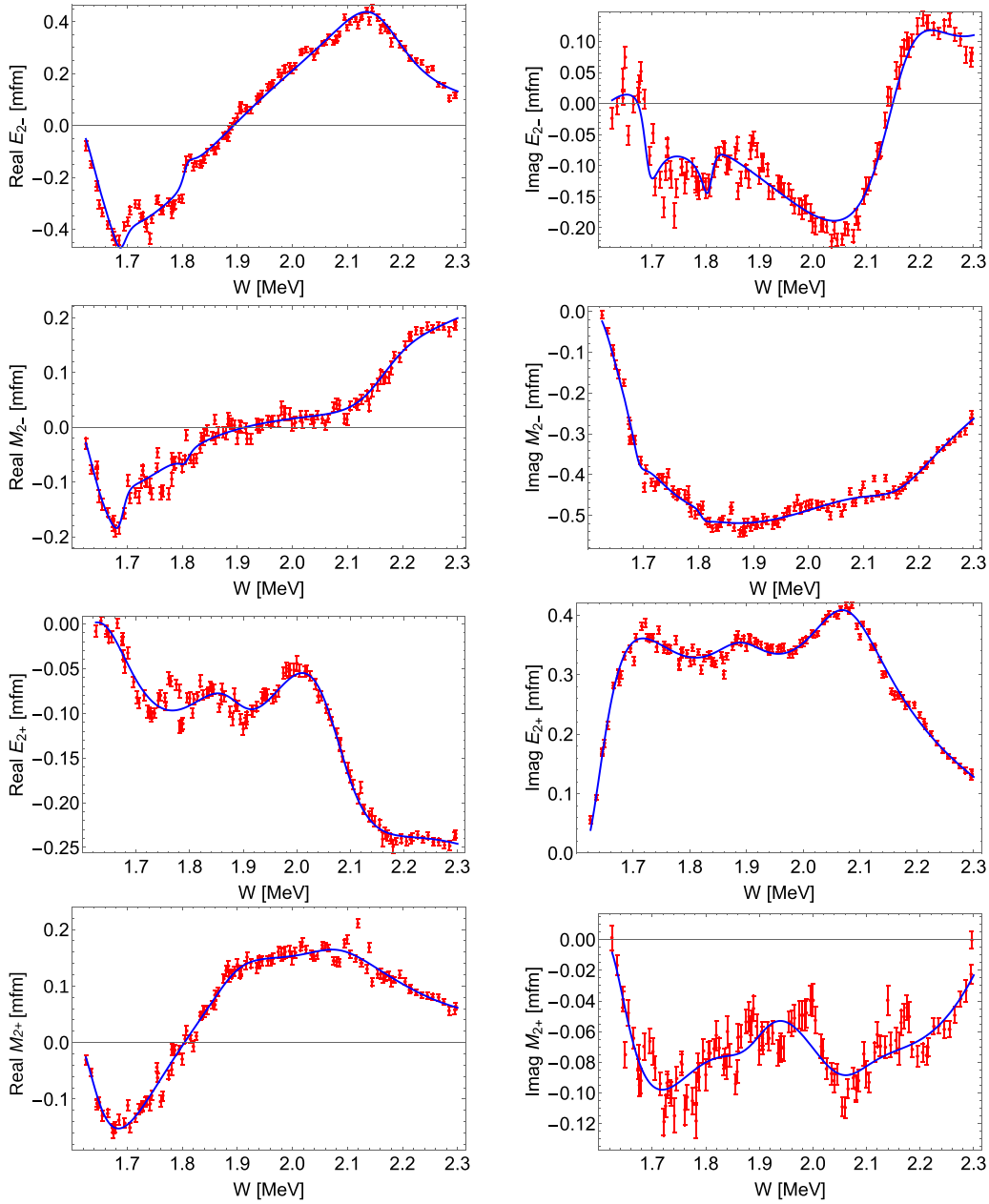

FIG. 12. Multipoles obtained from full L+P PWA of SE AA/PWA solutions. Red symbols are SE AA/PWA results, and full blue line is the full L+P fit. Pole results are given in Table II.

version of this work. Lothar Tiator found inconsistencies in early attempts and made suggestions for improvements; Yannick Wunderlich carefully read early versions of the manuscript and made suggestions which improved its consistency and precision. We hope these interactions continue and lead to future publications. A.S. acknowledges the support from the STRONG-2020 EU project, Grant Agreement No. 824093. This work was supported in part by the U.S. Department of Energy, Office of Science, Office of Nuclear Physics, under Grant No. DE-SC001652.

APPENDIX: FORMALISM FOR $K\Lambda$ PHOTOPRODUCTION

Partial-wave decompositions are introduced through Chew, Goldberger, Low, and Nambu (CGLN) amplitudes:

$$F_1(W,\theta) = \sum_{\ell=0}^{\infty}\{[\ell M_{\ell+}(W) + E_{\ell+}(W)]P'_{\ell+1}(\cos\theta) + [(\ell+1)M_{\ell-}(W) + E_{\ell-}(W)]P'_{\ell-1}(\cos\theta)\}, \tag{A1}$$

TABLE III. The definitions of the 16 polarization observables of pseudoscalar meson photoproduction are given here in terms of transversity amplitudes $b_1, \ldots, b_4$ (cf. Ref. [30]; sign conventions are consistent with [31]). Expressions are given both in terms of real and imaginary parts of bilinear products of amplitudes and in terms of moduli and relative phases of the amplitudes. Furthermore, the phase-space factor ρ has been suppressed in the given expressions (i.e., we have set $\rho = 1$). The four different groups of four observables each are indicated as well.

Observable	Group
$\sigma_0 = \frac{1}{2}(\lvert b_1\rvert^2 + \lvert b_2\rvert^2 + \lvert b_3\rvert^2 + \lvert b_4\rvert^2)$	$\mathcal{S}$
$\hat{\Sigma} = \frac{1}{2}(-\lvert b_1\rvert^2 - \lvert b_2\rvert^2 + \lvert b_3\rvert^2 + \lvert b_4\rvert^2)$	$\mathcal{S}$
$\hat{T} = \frac{1}{2}(\lvert b_1\rvert^2 - \lvert b_2\rvert^2 - \lvert b_3\rvert^2 + \lvert b_4\rvert^2)$	$\mathcal{S}$
$\hat{P} = \frac{1}{2}(-\lvert b_1\rvert^2 + \lvert b_2\rvert^2 - \lvert b_3\rvert^2 + \lvert b_4\rvert^2)$	$\mathcal{S}$
$\hat{E} = \mathrm{Re}[-b_3^* b_1 - b_4^* b_2] = -\lvert b_1\rvert\lvert b_3\rvert\cos\phi_{13} - \lvert b_2\rvert\lvert b_4\rvert\cos\phi_{24}$	$\mathcal{BT}$
$\hat{F} = \mathrm{Im}[b_3^* b_1 - b_4^* b_2] = \lvert b_1\rvert\lvert b_3\rvert\sin\phi_{13} - \lvert b_2\rvert\lvert b_4\rvert\sin\phi_{24}$	$\mathcal{BT}$
$\hat{G} = \mathrm{Im}[-b_3^* b_1 - b_4^* b_2] = -\lvert b_1\rvert\lvert b_3\rvert\sin\phi_{13} - \lvert b_2\rvert\lvert b_4\rvert\sin\phi_{24}$	$\mathcal{BT}$
$\hat{H} = \mathrm{Re}[b_3^* b_1 - b_4^* b_2] = \lvert b_1\rvert\lvert b_3\rvert\cos\phi_{13} - \lvert b_2\rvert\lvert b_4\rvert\cos\phi_{24}$	$\mathcal{BT}$
$\hat{C}_{x'} = \mathrm{Im}[-b_4^* b_1 + b_3^* b_2] = -\lvert b_1\rvert\lvert b_4\rvert\sin\phi_{14} + \lvert b_2\rvert\lvert b_3\rvert\sin\phi_{23}$	$\mathcal{BR}$
$\hat{C}_{z'} = \mathrm{Re}[-b_4^* b_1 - b_3^* b_2] = -\lvert b_1\rvert\lvert b_4\rvert\cos\phi_{14} - \lvert b_2\rvert\lvert b_3\rvert\cos\phi_{23}$	$\mathcal{BR}$
$\hat{O}_{x'} = \mathrm{Re}[-b_4^* b_1 + b_3^* b_2] = -\lvert b_1\rvert\lvert b_4\rvert\cos\phi_{14} + \lvert b_2\rvert\lvert b_3\rvert\cos\phi_{23}$	$\mathcal{BR}$
$\hat{O}_{z'} = \mathrm{Im}[b_4^* b_1 + b_3^* b_2] = \lvert b_1\rvert\lvert b_4\rvert\sin\phi_{14} + \lvert b_2\rvert\lvert b_3\rvert\sin\phi_{23}$	$\mathcal{BR}$
$\hat{L}_{x'} = \mathrm{Im}[-b_2^* b_1 - b_4^* b_3] = -\lvert b_1\rvert\lvert b_2\rvert\sin\phi_{12} - \lvert b_3\rvert\lvert b_4\rvert\sin\phi_{34}$	$\mathcal{TR}$
$\hat{L}_{z'} = \mathrm{Re}[-b_2^* b_1 - b_4^* b_3] = -\lvert b_1\rvert\lvert b_2\rvert\cos\phi_{12} - \lvert b_3\rvert\lvert b_4\rvert\cos\phi_{34}$	$\mathcal{TR}$
$\hat{T}_{x'} = \mathrm{Re}[b_2^* b_1 - b_4^* b_3] = \lvert b_1\rvert\lvert b_2\rvert\cos\phi_{12} - \lvert b_3\rvert\lvert b_4\rvert\cos\phi_{34}$	$\mathcal{TR}$
$\hat{T}_{z'} = \mathrm{Im}[-b_2^* b_1 + b_4^* b_3] = -\lvert b_1\rvert\lvert b_2\rvert\sin\phi_{12} + \lvert b_3\rvert\lvert b_4\rvert\sin\phi_{34}$	$\mathcal{TR}$

$$F_2(W,\theta) = \sum_{\ell=1}^{\infty}[(\ell+1)M_{\ell+}(W) + \ell M_{\ell-}(W)]P'_\ell(\cos\theta), \tag{A2}$$

$$F_3(W,\theta) = \sum_{\ell=1}^{\infty}\{[E_{\ell+}(W) - M_{\ell+}(W)]P''_{\ell+1}(\cos\theta) + [E_{\ell-}(W) + M_{\ell-}(W)]P''_{\ell-1}(\cos\theta)\}, \tag{A3}$$

$$F_4(W,\theta) = \sum_{\ell=2}^{\infty}[M_{\ell+}(W) - E_{\ell+}(W) - M_{\ell-}(W) - E_{\ell-}(W)]P''_\ell(\cos\theta). \tag{A4}$$

Transversity amplitudes are defined as

$$b_1(W,\theta) = -b_3(W,\theta) - \frac{1}{\sqrt{2}}\sin\theta \times \left[F_3(W,\theta)e^{-\imath\frac{\theta}{2}} + F_4(W,\theta)e^{\imath\frac{\theta}{2}}\right], \tag{A5}$$

$$b_2(W,\theta) = -b_4(W,\theta) + \frac{1}{\sqrt{2}}\sin\theta \times \left[F_3(W,\theta)e^{\imath\frac{\theta}{2}} + F_4(W,\theta)e^{-\imath\frac{\theta}{2}}\right], \tag{A6}$$

$$b_3(W,\theta) = \frac{\imath}{\sqrt{2}}\left[F_1(W,\theta)e^{-\imath\frac{\theta}{2}} - F_2(W,\theta)e^{\imath\frac{\theta}{2}}\right], \tag{A7}$$

$$b_4(W,\theta) = \frac{\imath}{\sqrt{2}}\left[F_1(W,\theta)e^{\imath\frac{\theta}{2}} - F_2(W,\theta)e^{-\imath\frac{\theta}{2}}\right]. \tag{A8}$$

All 16 polarization observables can be expressed in terms of transversity amplitudes; see Table III.

[1] A. Švarc, Y. Wunderlich, and L. Tiator, Phys. Rev. C **102**, 064609 (2020).
[2] A. Švarc, Y. Wunderlich, and L. Tiator, Phys. Rev. C **105**, 024614 (2022).
[3] S. Ciulli and J. Fischer, Nucl. Phys. **24**, 465 (1961).
[4] I. Ciulli, S. Ciulli, and J. Fisher, Nuovo Cimento **23**, 1129 (1962).
[5] E. Pietarinen, Nuovo Cimento A **12**, 522 (1972).
[6] E. Pietarinen, Nucl. Phys. B **107**, 21 (1976).
[7] A. Švarc, M. Hadžimehmedović, H. Osmanović, J. Stahov, L. Tiator, and R. L. Workman, Phys. Rev. C **88**, 035206 (2013).
[8] A. Švarc, M. Hadžimehmedović, H. Osmanović, J. Stahov, L. Tiator, and R. L. Workman, Phys. Lett. B **755**, 452 (2016).
[9] A. Švarc, M. Hadžimehmedović, R. Omerović, H. Osmanović, and J. Stahov, Phys. Rev. C **89**, 045205 (2014).
[10] A. Švarc, M. Hadžimehmedović, H. Osmanović, J. Stahov, L. Tiator, and R. L. Workman, Phys. Rev. C **89**, 065208 (2014).
[11] A. Švarc, M. Hadžimehmedović, H. Osmanović, J. Stahov, and R. L. Workman, Phys. Rev. C **91**, 015207 (2015).
[12] L. Tiator, M. Döring, R. L. Workman, M. Hadžimehmedović, H. Osmanović, R. Omerović, J. Stahov, and A. Švarc, Phys. Rev. C **94**, 065204 (2016).

[13] A. Švarc, Y. Wunderlich, H. Osmanović, M. Hadžimehmedović, R. Omerović, J. Stahov, V. Kashevarov, K. Nikonov, M. Ostrick, L. Tiator, and R. Workman, Phys. Rev. C **97**, 054611 (2018).
[14] A. Švarc, Y. Wunderlich, H. Osmanović, M. Hadžimehmedović, R. Omerović, J. Stahov, V. Kashevarov, K. Nikonov, M. Ostrich, L. Tiator, and R. Workman, Few-Body Syst. **59**, 96 (2018).
[15] P. A. Zyla *et al.* (Particle Data Group), Prog. Theor. Exp. Phys. **2020**, 083C01 (2020); and 2021 update, minireview on N and Δ resonances.
[16] A. V. Anisovich, V. Burkert, M. Hadžimehmedović, D. G. Ireland, E. Klempt, V. A. Nikonov, R. Omerović, H. Osmanović, A. V. Sarantsev, J. Stahov, A. Švarc, and U. Thoma, Phys. Rev. Lett. **119**, 062004 (2017).
[17] A. V. Anisovich, V. Burkert, M. Hadžimehmedović, D. G. Ireland, E. Klempt, V. A. Nikonov, R. Omerović, H. Osmanović, A. V. Sarantsev, J. Stahov, A. Švarc, and U. Thoma, Eur. Phys. J. A **53**, 242 (2017).
[18] Tests were carried out using a Lenovo Legion laptop with AMD Ryzen 7 4800H with Radeon Graphics processor, 2.90 GHz, and 16 Gb RAM with Mathematica 11.0 code. Shorter run times could be achieved using Fortran or C but Mathematica is a more versatile language for model testing.
[19] G. Höhler, Pion nucleon scattering, Pt. 2, in *Elastic and Charge Exchange Scattering of Elementary Particles*, Landolt-Bornstein, Pt. B (Springer-Verlag, Berlin, 1983), Vol. 9.
[20] H. Osmanović, M. Hadžimehmedović, R. Omerović, J. Stahov, V. Kashevarov, K. Nikonov, M. Ostrick, L. Tiator, and A. Švarc, Phys. Rev. C **97**, 015207 (2018).
[21] H. Osmanović, M. Hadžimehmedović, R. Omerović, J. Stahov, M. Gorchtein, V. Kashevarov, K. Nikonov, M. Ostrick, L. Tiator, and A. Švarc, Phys. Rev. C **100**, 055203 (2019).
[22] H. Osmanović, M. Hadžimehmedović, R. Omerović, J. Stahov, V. Kashevarov, M. Ostrick, L. Tiator, and A. Švarc, Phys. Rev. C **104**, 034605 (2021).
[23] See https://pwa.hiskp.uni-bonn.de.
[24] See https://gwdac.phys.gwu.edu.
[25] R. Bradford *et al.*, Phys. Rev. C **73**, 035202 (2006).
[26] M. E. McCracken *et al.*, Phys. Rev. C **81**, 025201 (2010).
[27] A. Lleres *et al.*, Eur. Phys. J. A **31**, 79 (2007).
[28] C. A. Paterson *et al.*, Phys. Rev. C **93**, 065201 (2016).
[29] P. Kroenert, Y. Wunderlich, F. Afzal, and A. Thiel, arXiv:2305.10367.
[30] W. T. Chiang and F. Tabakin, Phys. Rev. C **55**, 2054 (1997).
[31] Y. Wunderlich, Ph.D. thesis, University of Bonn, 2019, https://hdl.handle.net/20.500.11811/7868.